

Three-Dimensional Positioning Using EROS A Stereo Pairs

Tee-Ann TEO

Center for Space and Remote Sensing Research
National Central University, Chung-Li, TAIWAN
ann@csrsr.ncu.edu.tw

Liang-Chien CHEN

Center for Space and Remote Sensing Research
National Central University, Chung-Li, TAIWAN
lcchen@csrsr.ncu.edu.tw

ABSTRACT: This paper investigates the accuracy of three-dimensional positioning for EROS A stereo pairs when different numbers of ground control points are employed. The major works of the proposed schemes include: (1) initialization of orientation parameters (2) preliminary orbit fitting, (3) orbit refinement using the least squares filtering technique, and (4) space intersection. The experiment includes validation of positioning accuracy for an EROS A in-track stereo pair when different number of check points are employed.

KEY WORDS: EROS A Stereo Pairs, Orbit Adjustment, and Space Intersection.

1. INTRODUCTION

Three-dimensional positioning from remote sensing images is an important task for various remote sensing applications. EROS A is a high resolution imaging satellite. Its linear array pushbroom imager is with 1.8meter nadir resolution on ground. Using its body rotation capability, EROS A provides in-track stereo where stereo pairs are necessary for deriving in the same track. The objective of the work in this paper is three-dimensional positioning using EROS A stereo pairs when different number of check points are employed. The central tasks include (1) initialization of orientation parameters, (2) preliminary orbit fitting, (3) orbit

refinement using least squares filtering technique, and (4) space intersection.

2. ORBIT ADJUSTMENT

The major step in validating the positioning accuracy for an image is to model the orbit parameters and the attitude data. Due to the extremely high correlation between two groups of orbital parameters and attitude data, we only correct the orbital parameters. That means we will use the attitude information in the on-board ephemeris data as known values. Three steps are included in orbit adjustment. The first step is to initialize the orientation parameters using on-board ephemeris data. We then fit the orbital parameters with second-degree polynomials using GCPs. Once the trend functions of the orbital parameters are determined, the fine-tuning of an orbit is performed by using Least Squares Filtering technique.

2.1. Initialization of Orientation Parameters

The on-board ephemeris data and GCPs are in different coordinate systems. Before the orbit adjustment, it is essential to build up the coordinate transformation, so that the orbit adjustment will be performed in WGS84 as unified coordinate systems. Those coordinate systems include inertial frame, WGS84,

GRS67, Geodetic Coordinate System, TWD67, Orbital Reference Frame and EROS A Body Frame. In which GRS67 uses the Kaula ellipsoid ($a=6378160m$, $f=1/298.247$). The camera model is provided by satellite company.

2.2. Preliminary Orbit Fitting

Because the on-board data includes errors to a certain degree, GCPs are needed to adjust the orbit parameters. Referring to figure 1, the observation vector (U_a) provided by the satellite will not pass through the corresponding GCP due to errors in the on-board data [1]. Thus, correction of the orbit data from (x_0, y_0, z_0) to (x, y, z) may be performed under conditions when:

$$\begin{aligned} X_i &= x(t_i) + S_i u_{xi} \\ Y_i &= y(t_i) + S_i u_{yi} \\ Z_i &= z(t_i) + S_i u_{zi} \end{aligned} \quad (1)$$

$$\begin{aligned} x(t_i) &= x_0 + a_0 + a_1 \cdot t_i + a_2 \cdot t_i^2 \\ y(t_i) &= y_0 + b_0 + b_1 \cdot t_i + b_2 \cdot t_i^2 \\ z(t_i) &= z_0 + c_0 + c_1 \cdot t_i + c_2 \cdot t_i^2 \end{aligned} \quad (2)$$

Where, X_i, Y_i, Z_i are object coordinates of the i^{th} GCP, u_{xi}, u_{yi}, u_{zi} are components of the observation vector, $x(t_i), y(t_i), z(t_i)$ are the satellite's coordinates of the i^{th} GCP after correction, x_0, y_0, z_0 are the satellite's coordinates before correction, a_i, b_i and c_i ($i=0,1,2$) are coefficients for orbit corrections, t represents sampling time, and S_i is the scale factor.

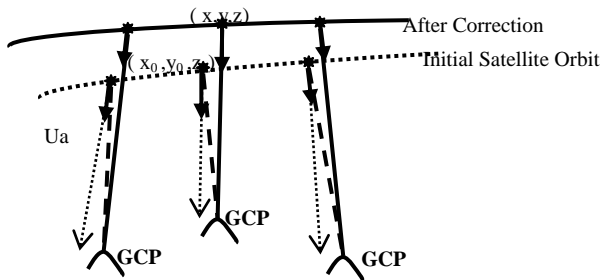


Fig. 1. Preliminary fitting for of satellite orbit

2.3. Least Squares Filtering

Because the least squares adjustment is a global

treatment, it cannot correct for the local errors. Therefore, the least squares filtering [2] has to be used to fine tune the orbit. By doing this, we assume that the x, y, z -axis are independent. Thus, we use three one-dimensional functions to adjust the orbit. The model of least squares filtering is shown as

$$\rho_k = \vec{v}_k \left[\sum_k \right]^{-1} \vec{\epsilon}_k \quad (3)$$

Where, k is x, y, z axis, \vec{v}_k is the correction value of the interpolating point, \vec{v}_k is the row covariance matrix of the interpolating point with respect to GCPs, \sum_k is the covariance matrix for GCPs, and $\vec{\epsilon}_k$ is the residual vectors for GCPs.

The basic consideration in this investigation is to minimize the number of required GCPs. Thus, using a large amount of GCPs to characterize the covariance matrix is not practical. In this paper, we use a Gaussian function with some empirical values as the covariance function. The Gaussian function is shown as

$$\text{Covariance} = \begin{cases} (1 - r_n) \mu_k e^{-2.146 \frac{d}{d_{\max}}}, & \text{if } d \neq 0 \\ \mu_k, & \text{if } d = 0 \end{cases} \quad (4)$$

Where, d is the distance between an unknown points and a GCP, d_{\max} is the distance between an unknown point and the farthest GCP, μ_k is the variance of GCPs' residual, and r_n is the filtering ratio, in which we use $r_n = 0.1$ in experiment. The empirical value 2.146 is selected so that the covariance is limited to 1% of $0.01(1 - r_n) \mu_k$ when $d = d_{\max}$ [3].

3. SPACE INTERSECTION

A space intersection is performed when the orbit and attitude parameters of a stereo pair are determined. Referring to fig 2, an image points can built up 3 equations by using the equation of line. Thus, six equations may be formulated for a point pair. By employing least squares adjustment, the intersection point will be determined by solving equation 5.

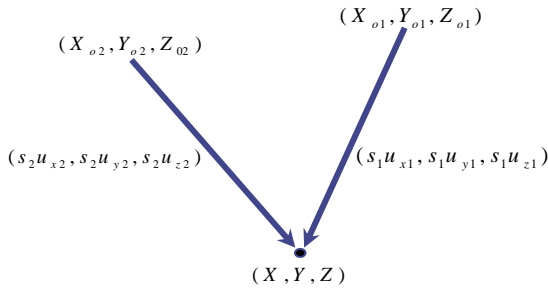


Fig. 2. Illustration of Space Intersection

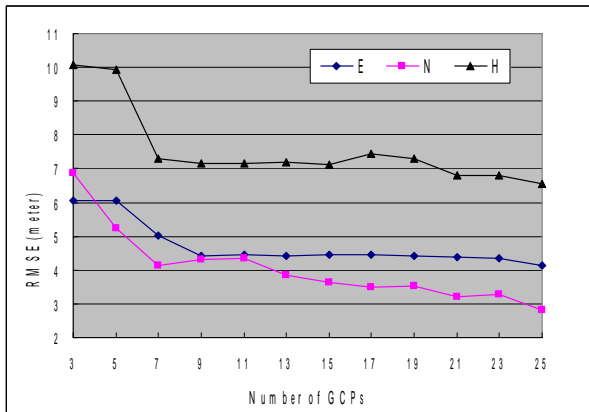
$$\begin{aligned}
 X &= X_{o1} + S_1 u_{X1} \\
 Y &= Y_{o1} + S_1 u_{Y1} \\
 Z &= Z_{o1} + S_1 u_{Z1} \\
 X &= X_{o2} + S_2 u_{X2} \\
 Y &= Y_{o2} + S_2 u_{Y2} \\
 Z &= Z_{o2} + S_2 u_{Z2}
 \end{aligned}$$

(5)

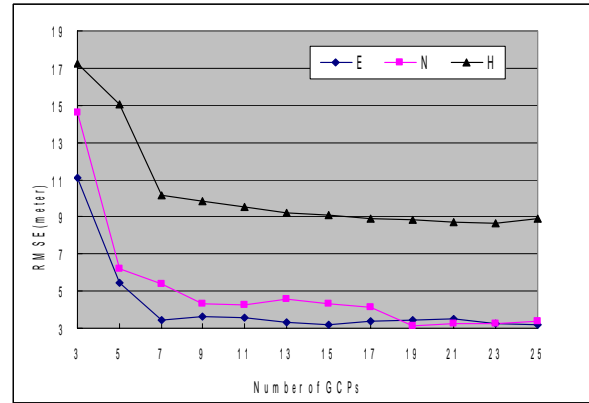
4. EXPERIMENTAL RESULTS

The test data includes two sets of in-track stereo pairs, which were sampled on November 29, 2001 and March 11, 2002, respectively. The base-to-height ratio is about 0.43 in the first case and the second pair has a ratio of 0.38. Both cases are with 90% overlap. The asynchronous ratio is 1:10 and 1:5. The ground coordinates for 49 conjugate points were manually measured from 1/1000 scale topographic map.

Figure 5 indicates the RMSEs of CHKPs when different numbers of GCPs were employed in the test data. It is obvious that the RMSEs tend to be stable when 9 or more control points were employed. The RMSEs for the CHKPs when using 9 GCPs are shown in Table 1.



(a) Case A



(b) Case B

Fig. 3. RMSE of Check Points with Different Numbers of GCPs

Table 1. RMSE of Space Intersection

	GCP (9)			CHKP (40)		
Unit:	RMSE	RMSE	RMSE	RMSE	RMSE	RMSE
meter	E	N	H	E	N	H
Case A	3.41	4.32	2.36	4.43	4.32	7.17
Case B	3.10	3.87	2.98	3.63	4.29	9.82

5. CONCLUSIONS

This paper investigates 3-D positioning accuracy for EROS A stereo pairs. Experimental results indicate that, for a EROS A in-track stereo pairs with 0.4 base-to-height ratio when 9 GCPs are used, the horizontal accuracy is better than 4.5 m. While the vertical accuracy ranges from 7m to 10m.

REFERENCES

- [1] Chen, L.C. and T.A. Teo, 2001, Orbit Adjustment for EROS A1 High Resolution Satellite Images, Proceeding of 22nd Asian Conference on Remote Sensing, Singapore, pp1169-1174.
- [2] Mikhail E.M and Ackermann F., 1982, Observation and Least Squares, University Press of America, New York, pp.401.
- [3] Chen, L.C. and L.Y. Chang, 1998, Three Dimensional Positioning Using SPOT Stereostrips with Sparse Control, Journal of Surveying, ASCE 124(2): pp.63-72.